Article

On the Properties Evolution of Eco-Material Dedicated to Manufacturing Artificial Reef via 3D Printing: Long-Term Interactions of Cementitious Materials in the Marine Environment

Fouad Boukhelf [1,*], Nassim Sebaibi [1], Mohamed Boutouil [1], Adrian I. Yoris-Nobile [2], Elena Blanco-Fernandez [2], Daniel Castro-Fresno [2], Carlos Real-Gutierrez [2], Roger J. H. Herbert [3], Sam Greenhill [3], Bianca Reis [4,5], João N. Franco [4,5,6], Maria Teresa Borges [4,5], Isabel Sousa-Pinto [4,5], Pieter van der Linden [4,5], Oscar Babé Gómez [4,5], Hugo Sainz Meyer [4,5], Emanuel Almada [4,5,7], Rick Stafford [3], Valentin Danet [8], Jorge Lobo-Arteaga [9,10], Miriam Tuaty-Guerra [5,9] and Alice E. Hall [11]

1   Laboratoire de Recherche ESITC Caen, Communauté de la Normandie Université, 1 Rue Pierre et Marie Curie, 14610 Epron, France; nassim.sebaibi@esitc-caen.fr (N.S.); mohamed.boutouil@esitc-caen.fr (M.B.)
2   Grupo GITECO, Universidad de Cantabria, 39005 Santander, Spain; adrianisidro.yoris@unican.es (A.I.Y.-N.); elena.blanco@unican.es (E.B.-F.); daniel.castro@unican.es (D.C.-F.); carlos.real@unican.es (C.R.-G.)
3   Department of Life and Environmental Sciences, Bournemouth University, Talbot Campus, Fern Barrow, Poole BH12 5BB, UK; rherbert@bournemouth.ac.uk (R.J.H.H.); greenhills@bournemouth.ac.uk (S.G.); rstafford@bournemouth.ac.uk (R.S.)
4   Faculdade de Ciências, Universidade do Porto, Rua do Campo Alegre s/n, 4150-181 Porto, Portugal; r.biancareis@gmail.com (B.R.); jfranco@zoo.uc.pt (J.N.F.); mtborges@fc.up.pt (M.T.B.); isabel.sousa.pinto@gmail.com (I.S.-P.); lindenvdpieter@gmail.com (P.v.d.L.); oscarbabegomez@gmail.com (O.B.G.); sainzmeyerhugo@gmail.com (H.S.M.); emanueldealmada@gmail.com (E.A.)
5   CIIMAR—Centro Interdisciplinar de Investigação Marinha e Ambiental, Terminal de Cruzeiros do Porto de Leixões, Av. General Norton de Matos s/n, 4450-208 Matosinhos, Portugal; mguerra@ipma.pt
6   MARE—Marine and Environmental Sciences Centre, Escola Superior de Turismo e Tecnologia do Mar , Politécnico de Leiria, 2520-620 Peniche, Portugal
7   MARE—Marine and Environmental Sciences Centre, Quinta do Lorde Marina, Sítio da Piedade, 9200-044 Madeira, Portugal
8   Muséum National d'Histoire Naturelle, Station Marine de Dinard, CRESCO, 35800 Dinard, France; valentin.danet@mnhn.fr
9   Instituto Português do Mar e da Atmosfera, I.P., Divisão de Oceanografia e Ambiente Marinho, Rua Alfredo Magalhães Ramalho 6, 1495-006 Lisboa, Portugal; jorge.arteaga@ipma.pt
10 MARE—Centro de Ciências do Mar e do Ambiente, Campus de Caparica, Universidade Nova de Lisboa, 2829-516 Caparica, Portugal
11 School of Biological and Marine Sciences, Marine Institute, Plymouth University, Drake Circus, Plymouth PL4 8AA, UK; alice.hall@plymouth.ac.uk
*   Correspondence: fouad.boukhelf@esitc-caen.fr; Tel.: +33-231-463-202

Abstract: This paper deals with the evolution monitoring of biomass colonization and mechanical properties of 3D printed eco-materials/mortars immersed in the sea. Measurements of tensile strength, compressive strength, and Young's modulus were determined on samples deployed along the Atlantic coast of Europe, in France, United Kingdom, Spain, and Portugal. The samples were manufactured using 3D printing, where six mix designs with a low environmental impact binder were used. These mortars were based on geopolymer and cementitious binders (Cement CEM III), in which sand is replaced by three types of recycled sand, including glass, seashell, and limestone by 30%, 50%, and 100% respectively. The colonization of concrete samples by micro/macro-organisms and their durability were also evaluated after 1, 3, 6, 12, and 24 months of immersion. The results showed that both biomass colonization and mechanical properties were better with CEM III compared to geopolymer-based compositions. Therefore, the mixed design optimized according to mechanical properties show that the use of CEM III should be preferred over these geopolymer binders in 3D printed concrete for artificial reef applications.

1. Introduction

Since the Roman Empire and ancient Greece, artificial reefs (AR) were built for strategic military purposes, such as maritime blockades or to damage and sink enemy ships [1]. Nevertheless, artificial reefs now have more specific purposes related to the restoration of fisheries resources and ecosystem biodiversity, and their deployment often aims to mitigate the effects of resource exploitation, including destructive practices such as trawling [2]. As marine biodiversity provides beneficial ecosystem services such as commercial fisheries and tourism, particularly recreational underwater diving [3,4], it is imperative to conserve and restore marine ecosystems. Increased knowledge of artificial reef design and deployment is also being applied to the ecological enhancement of other coastal structures [5]. To summarize, Figure 1 shows the different countries represented in dark color that have artificial reefs.

Moreover, natural reefs (NR) are considered one of the most diverse ecosystems on Earth. Natural reefs have been disappearing due to a combination of factors such as overfishing, pollution, and pathogen decreases. However, this problem can be minimized by developing artificial reefs capable of attracting as much biodiversity as natural reefs, improving not only the environment, but also the economy. In Europe, most of the artificial reefs have been developed in the Mediterranean Sea (in France, they represent 95% of the total artificial reefs) and they have commonly been constructed with concrete to ensure a high level of stability and allow the realization of modules of various shapes and sizes. However, although many reef deployment such as Nienhagen, Germany, in 2003 [6], Pedaso, Italy, in 2005 [7], Bay of Marseilles, France, in 2008 [8], and Nazaré, Portugal, between 1990 and 2010 [9] show an improvement in the biodiversity, the materials generally used are not sustainable due to the high carbon footprint of Portland cement (commonly used to fabricate concrete).

Moreover, the techniques used to manufacture AR is the common framework system which does not allow the reproduction of NR contours. Moreover, innovations of "3DPARE" project are new sustainable materials designed specifically to enhance marine life and marine biodiversity; new construction techniques, a 3D printer, capable of reproducing the enormous variety of Atlantic marine and coastal environments; and original and innovative approaches combining several thematic (materials science, marine science, and 3D numerical modeling).

In fact, additive manufacturing is a technology developed in the 1980s [10] which can be defined as "the process of joining materials to create objects from three-dimensional (3D) model data, usually layer by layer". This technology reduces product design constraints through its flexibility, its ability to produce shapes with complex geometries, and its process optimization. All these advantages increase the functionality of the product and thus reduce the amount of energy, fuel, and natural resources required for production [11]. Programming and numerical optimization make it possible to optimize the various elements to be produced upstream and thus to use the raw material efficiently while generating a minimum of waste [10,12].

Additive manufacturing enables new developments in the sector of constructions based on cementitious materials, in terms of the complexity of shapes, the possibility of building elements without formwork and the associated cost reductions, the possibility of building in highly polluted environments without endangering human beings, and to consider the construction for settlement in space [13,14]. The most common method of digital concrete manufacturing is based on 3D printing technology [15].

Many studies and projects have developed 3D printers on industrial and site scales [14,16]. In order to do so, several constraints must be overcome [14,17–19]. The first type of constraint

is related to the 3D printing manufacturing process: ensuring the bond between the layers, the size of the shapes which is related to the dimensions of the printer, and ensuring the stability of the object during and after printing. The second type of constraint concerns the formulations used for the material, which must meet different criteria: pumpability, extrudability, constructability, workability, and mechanical resistance. The addition of these constraints generates a paradox: the formulation must be sufficiently fluid to pass through the print head [20], but also stiff enough to support its own weight and that of the upper layers, while ensuring the mechanical stability of the structure.

Figure 1. Countries possessing artificial reefs, Céplamar report online, 21 April 2015 [21].

The 3DPARE project is part of the environmental transition recommending the use of materials with low environmental impact and advanced construction techniques notably 3D printing and its main goal to improve marine species colonization by encouraging greater diversity and biomass. For this purpose, ARs are manufactured with several complex forms designed to mimic a habitat that will attract marine life. The realization of these complex-shaped reefs requires a highly advanced manufacturing technique which is 3D printing. Moreover, knowledge of the durability properties of the materials used is of primary importance to realize a resistant and durable reef that withstands the aggressive marine environment. The objective of this study is to investigate the durability properties of materials vis-à-vis the marine environment at the material scale. This has been achieved by monitoring the mechanical properties and biomass colonization of cementitious materials compatible with 3D printing. Firstly, different materials with substitutes (binder and fine aggregates) were made in Spain and immersed in four different areas (France, Portugal, Spain, and the United Kingdom). Secondly, the characterization of the colonized biomass on the surface of the samples as well as the mechanical properties were studied at different ages (1, 3, 6, 12, and 24 months). The characterization protocol in the hardened state is presented below. The optimal composition will contribute to life cycle analysis to decide which formulation should be used to create 3D printed AR.
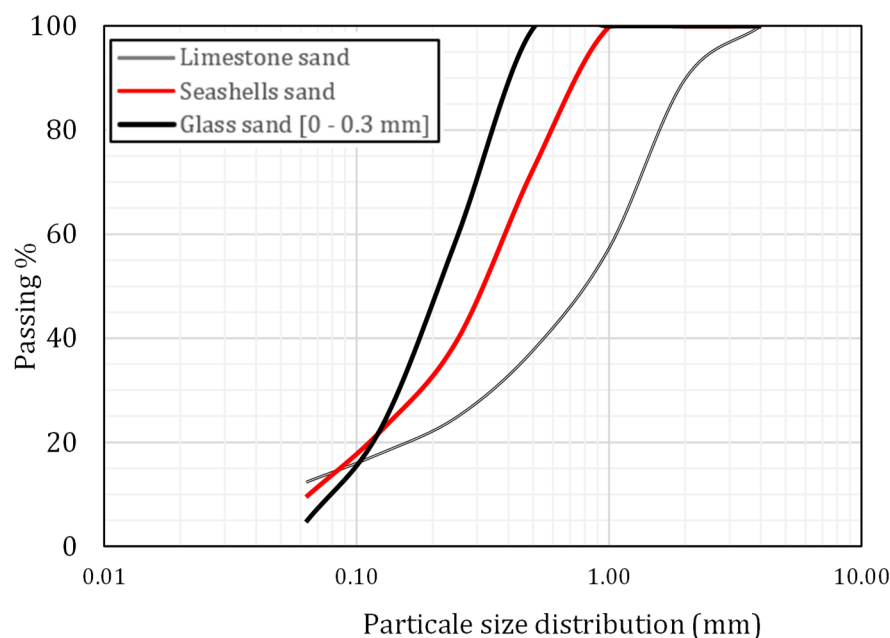
2. Experimental Program

2.1. Raw Materials

To assess the effect of binder and filler on the mechanical and durability properties, six mortars containing geopolymer and cement binders were analyzed. In fact, the geopolymer binder (G) was manufactured with fly ash as the main binder, sodium hydroxide (14 M of NaOH) for the alkaline activation, and the cement used (C) is a CEM. III/B 32.5 N-SR containing 31% of clinker and 66% of steel slag. The mineralogical composition of CEM III used is showed in Table 1.

Table 1. Mineralogical composition of CEM III used.

Composition	C3S	C2S	C3A	C4AF
CEM III/B	67%	11%	10%	8%

The acronyms attributed to the formulations were as follow: GL, GG, and GS refer to mortar with geopolymer binder based on fly ash (592.5 kg/m^3) and NaOH as an alkaline activator (267 kg/m^3) + water (26.7 kg/m^3) + a partial mass replacement of fine aggregate by 30% of glass sand, 50% of seashell sand, or 100% of limestone, respectively; whereas CL, CG, and CS mean mortar based on cement (521.6 kg/m^3) + water (278.5 kg/m^3) fly ash and kaolin as additions (260.8 and 21.7 kg/m^3, respectively) + the same fine aggregates used for the geopolymer mortars, respectively. The particle size analysis of the sands used is shown in Figure 2. Indeed, the glass powder presents a higher fineness than the other types of fine aggregates.

Figure 2. Granulometric analysis of sands used.

To obtain a similar printability for all the tested formulations, the rheology is the first criterion to be respected. The superplasticizer is used in the cement-based formulations and varies from 3.7, 4.4, and 3 kg/m^3 for CL, CS, and CG respectively. Indeed, the rheology was tested by means of a torque rheometer. The rheology results of the mortars studied show a linear behavior represented by the Bingham model ($\tau = \eta \times \dot{\gamma} + \tau_0$) such that the slope $\eta \approx 15$ Pa/s and it shows the plastic viscosity and $\tau_0 = 300$ Pa represents the initial shear stress. These results were reported in [22].

2.2. Sample Manufacturing

The fresh mortars were poured to prepare the samples via 3D printer type Delta-WASP 3MT based on EMS technology. The pouring was done layer by layer in order to produce blocks whose maximal printing volume is 1 m by edge. In this case study, plates manufactured measured $40 \times 51 \times 6.4$ cm. These plates were divided to create 20 prismatic specimens of $4 \times 4 \times 16$ cm. Our printer has a head composed of a nozzle and a 3-axis screw wheel inside which, by turning, via an electric motor, drains the material to be printed towards the nozzle (cf. Figure 3a). In our study, mortar plates were printed with the six formulations selected as defined below. After several preliminary sensitivity tests in terms of printing speed and orientation, nozzle diameter and mixing speed of the fresh mortar

contained in the printer tank and their impact on the final shape of the printed plates, the different parameters given below are recommended for 3D printing using this type of material. In fact, the printing process starts with the wall line of the entire perimeter of the plate. After that, there is the filling phase where the area was filled with lines inclined at 45° which alternate layer after layer (cf. Figure 3b). Moreover, the nozzle used for printing had a diameter of 20 mm, the speed of the printed head was limited to 100–300 mm/s and the rotation speed of the worm drive dedicated to extruding the fresh mortars varied in the range 100–300 rpm depending on the speed of printed head and the zone to be printed as shown in Figure 3c,d.
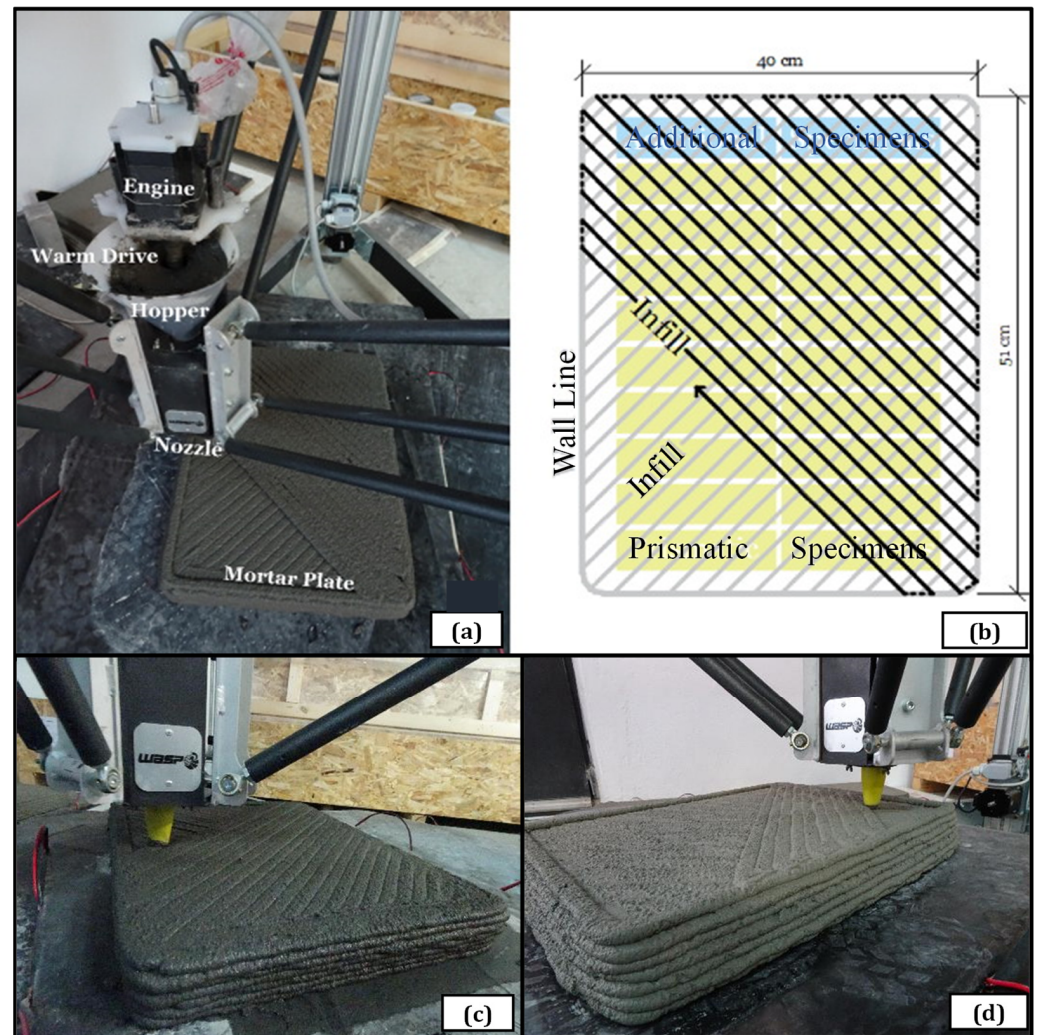

Figure 3. 3D printer detail (**a**), mortar plate printed and cutting scheme (**b**) [23], and plate printed in fresh state (**c**,**d**).

After curing in the air of the laboratory environment, in which the temperature and relative humidity ranged from 15.7 to 18.3 °C and 42.9 to 69% between night and day, respectively, the resulting plates were cut into 20 prismatic specimens using a saw with a diamond disk and respecting the printing orientation (cf. Figure 4). Once the cutting was completed, the upper printing face of the prismatic specimens were identified and arranged on the platform to be immersed, with a distance of 1 cm of space between and below the samples.
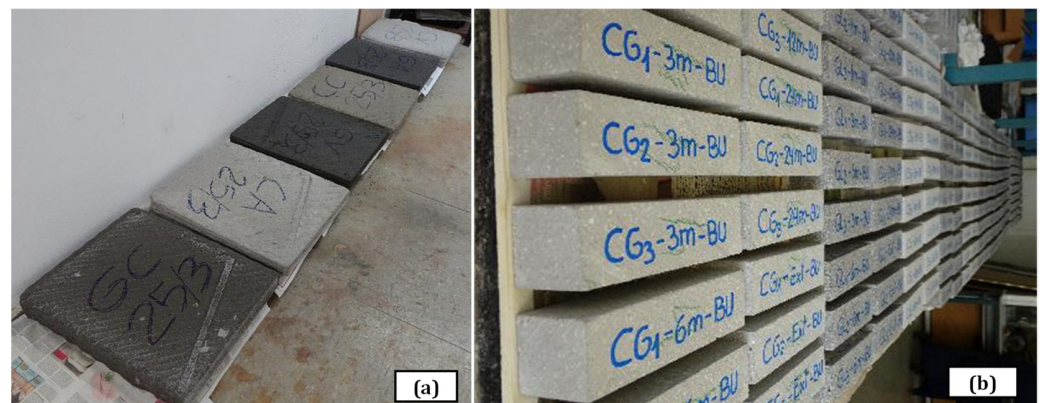
Figure 4. (**a**) Printed plates. (**b**) Samples are cut, referred, and organized before being delivered to the immersions areas.

2.3. Immersion and Monitoring

For logistical reasons, we chose small prismatic samples (4 × 4 × 16 cm) to facilitate the transport between the international partners of the project and to be able to easily recover the samples immersed in the different immersion areas and then return them to ESITC Caen for an eventual characterization in the laboratory. The distribution of prismatic specimens was as follows: four partners (France FR, Spain SP, Portugal PT, and United Kingdom UK); six different formulations; five immersion periods (1, 3, 6, 12, and 24 months); three replicates per formulation. This led to a total of 540 prismatic specimens regrouped and fixed as shown in Figure 5. Then, samples were immersed in the four immersion zones shown in Figure 6. More precisely, the depth of the immersion area was about 1.2 m of depth in the Deportivo Harbor at 43°27′44.6″ N 3°47′42.0″ W for the Spanish immersion, in the open sea in front of the bay of Saint Malo at 48°39′18.47″ N, 2°03′39.61″ W and at 6 m depth for the French immersion, at 3 m depth near to the Poole Harbor in the United Kingdom at 50°42′32.1″ N 1°59′11.1″ W, and 3 m depth near to the Matosinhos Harbor in Portugal at 41°10′35.1″ N 8°42′14.2″ W. After the immersion period, samples were recovered containing biomass colonization as shown in Figure 7 from Poole Harbor in the UK.
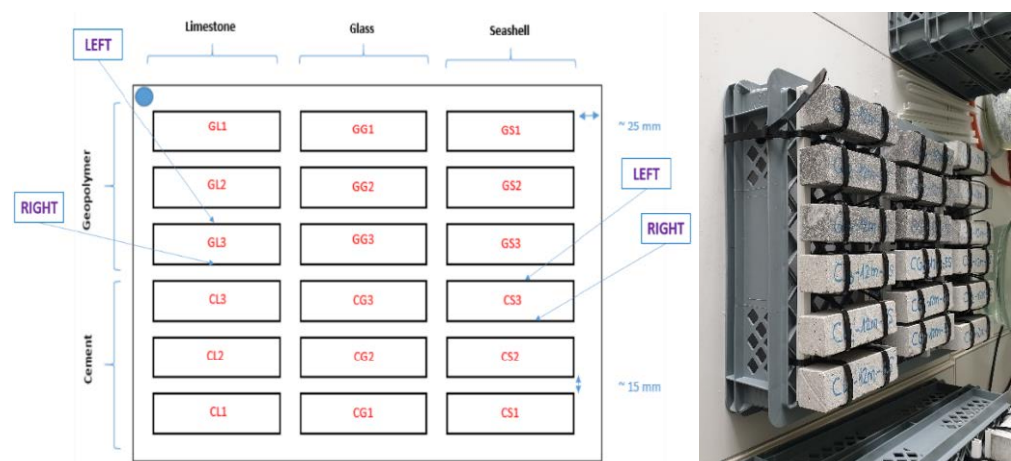

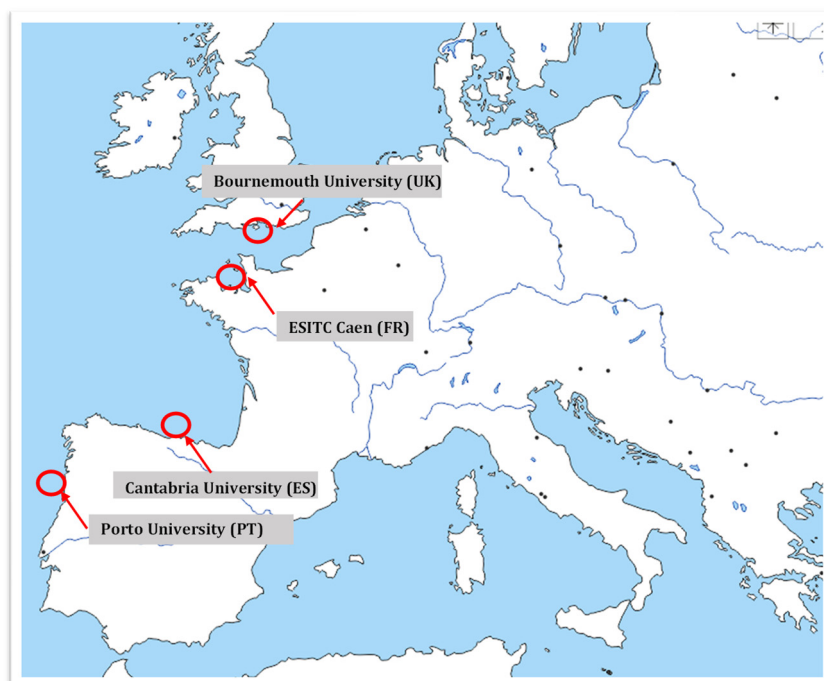**Figure 5.** Positions and fixation of the samples in the cages.

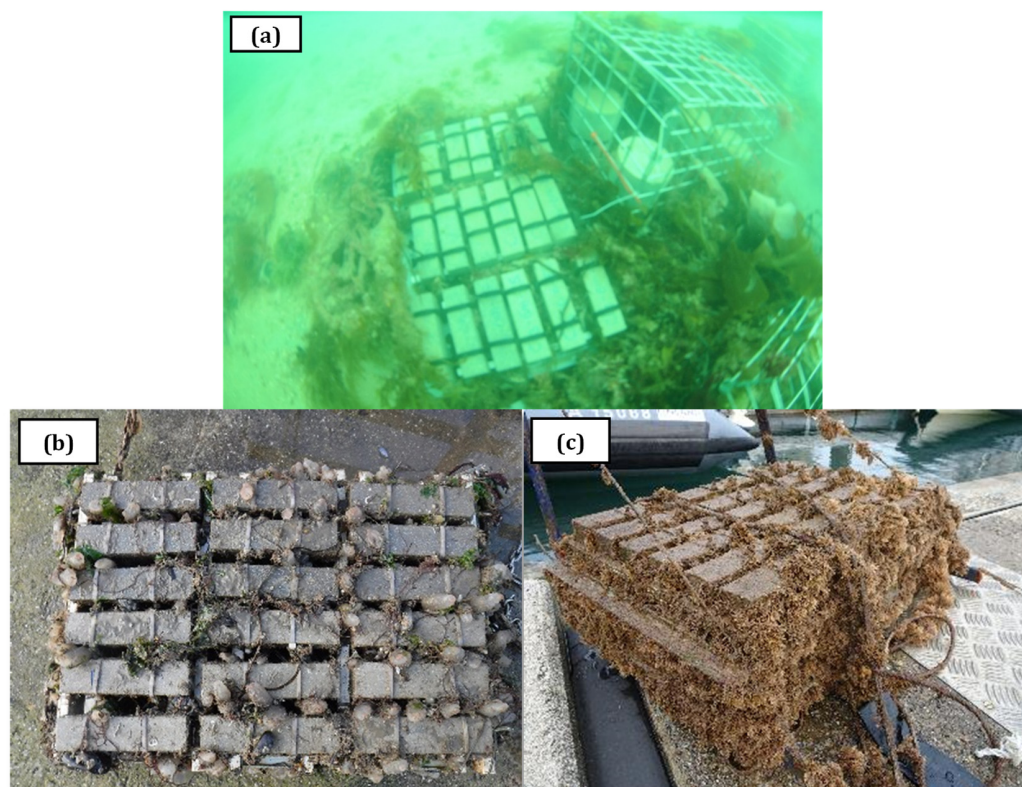**Figure 6.** The project partners' institutions and nearby immersion zones.

Figure 7. (**a**) Samples immersed in the United Kingdom area. (**b**,**c**) Biomass colonized after 1 month and 3 months of immersion, respectively.

2.4. Experimental Protocol

After receiving the samples at the laboratory, each sample was manually scrubbed with a brush under distilled water with the purpose of scraping and collecting all micro- and macro-organisms attached to the sample surfaces. The water used in this process

containing the biomass was then filtered through 25 μm filter papers to retain organisms (cf. Figure 8) which were weighed after being dried at 105 °C. Wet mass of the filters was noted. This mass is measured according to the protocol at wet state reported by Ly et al. [23]. We were able to collect the results of the biomass at different locations and at different deployment ages. The mechanical properties of specimens were investigated according to the French standard EN 196-1 [24]. The corresponding loading rates of the compressive and flexural strength were 2400 ± 200 N/s and 50 ± 10 N/s, respectively. Indeed, the sample size was 4 × 4 × 16 cm for the flexural strength and 4 × 4 × 4 for the compressive strength and Young's modulus. These two were measured simultaneously.
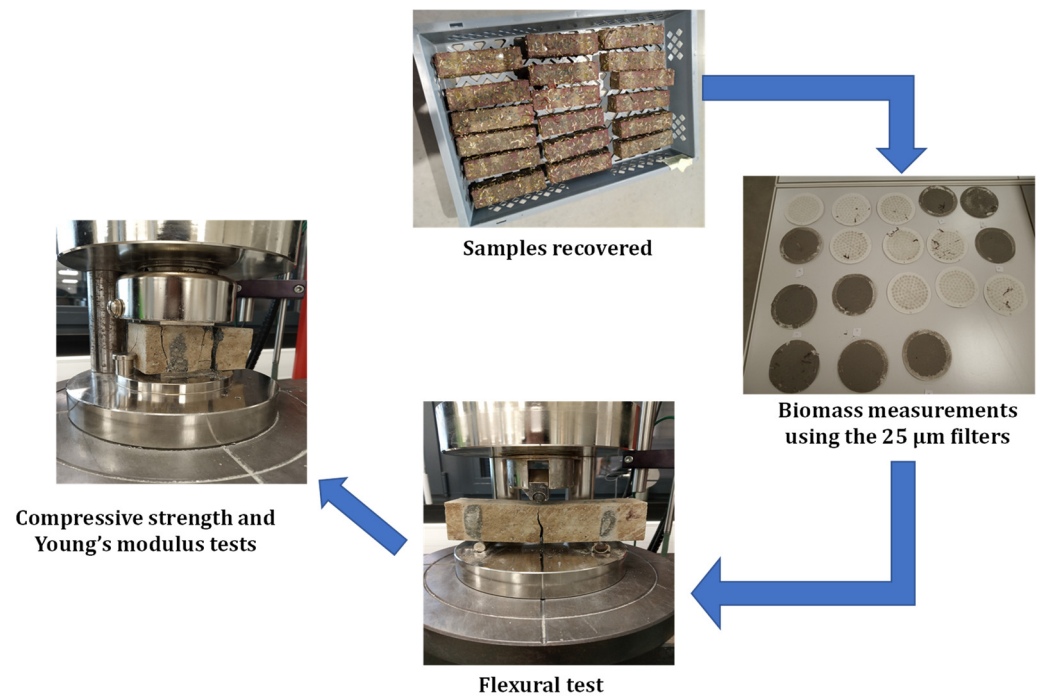

Figure 8. The approach taken in this study.

3. Results and Discussion

3.1. Biomass Weights Results of All Immersion Time

Figure 9 shows an increase in biomass of 8, 15, and 48 times after 3, 6, and 12 months, respectively, compared with the results after 1 month of immersion. Nevertheless, this parameter decreased after 24 months of immersion by 58% compared to the results of 12 months of immersion. Regrettably, the French samples dedicated to the study after 24 months of immersion were lost due to seabed movements. In general, the biofouling which is characterized by the mass colonization was different depending on the immersion region. In fact, the biomass was much higher in the southern part of the Atlantic (Portuguese and Spanish northern coasts) compared to its northern part (British and French coasts). Results may appear mitigated for French samples, for which the colonization was visually difficult to assess [23]. In fact, seawater is a complex environment and salinity depends on the region [25]. The chemical composition of seawater together with the variation in immersion depth could affect the pH of samples and influence the bio-colonization [26]. The average biomass measurement versus the time of immersion is shown in Figure 10. The regression curves with an R^2 of nearly 1 are also plotted using a polynomial distribution of degree 2. Indeed, the formulations CL, CS, GL, and GS presented maximum values after one year of immersion. Beyond that, a decrease was observed. Concerning the CG and GG formulations, the colonized biomass did not stop increasing with the immersion time.
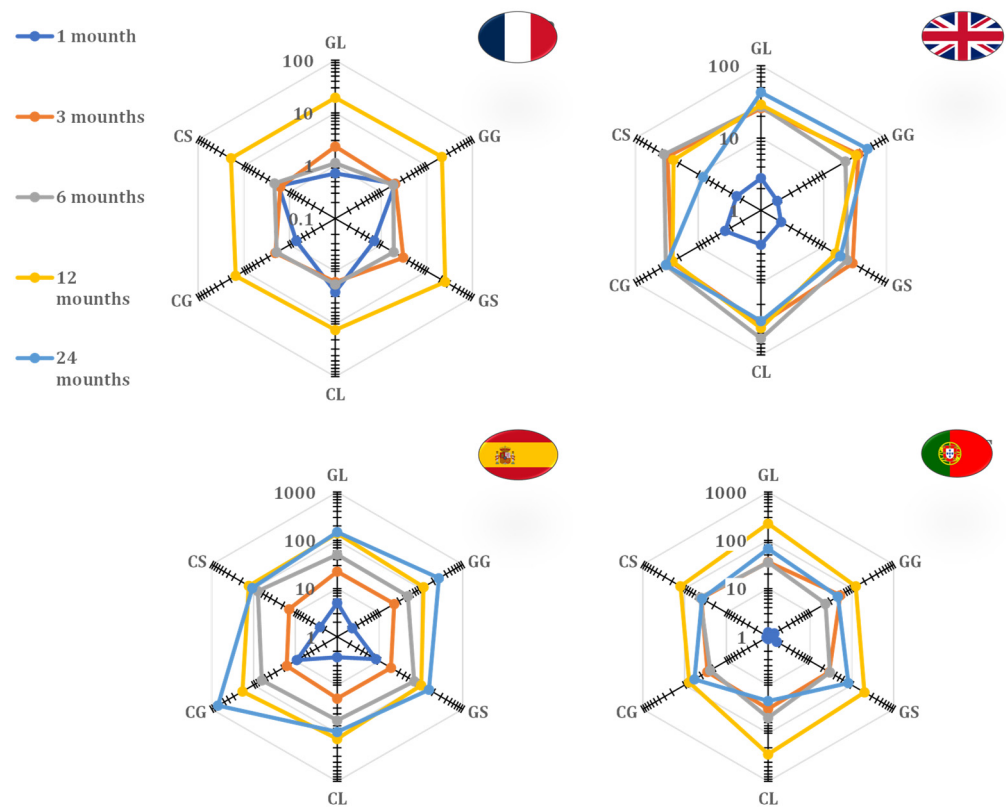
Figure 9. Biomass values at 1, 3, 6, 12, and 24 months.

3.2. Mechanical Properties Results

Concerning the mechanical results, we observed that the CL and CG formulation presents the maximum values in tensile/compressive strengths and Young's modulus. This can be explained by the pozzolanic reaction on portlandite with the silica contained in limestone and glass [27,28]. In addition, a decrease in these three parameters was also observed according to the formulations used, in this case the CS, GL, GG, and GS respectively. An increase of the tensile strength was noticed according to the immersion age at the sites in Portugal, the United Kingdom, and Spain, contrary to France which presented a decrease (cf. Figure 11). In addition, a good agreement between the results of the compression strength and those of the tensile strength was observed. Indeed, the CEM III/B cement used contained 33% clinker plus ground granulated blast furnace slag (GGBS). This cement type is particularly recommended for marine environments due to its microstructure after hydration. Moreover, seawater is the transport vector for aggressive agents that affect the properties of materials notably the calcium silica hydrate (CSH) formation and alter durability [29]. It contains mainly dissolved sodium chloride and magnesium sulfate. These can lead to the formation of secondary ettringite and secondary gypsum and thus cause expansion and damage to the concrete. However, CEM III/B presents a good resistance to sulfate attack [30] due to a denser microstructure and its high amount of blast furnace slag (>66%) which give reducing conditions in the pore solution [31]. This interstitial solution is strongly alkaline of order > 13, which is favorable for maintaining $Ca(OH)_2$ precipitation despite a lower hydroxyl (OH^-) concentration [30]. GGBS hydrates more slowly than Portland clinker and the increase in compressive strength occurs later in the curing process [32]. In the very long term, the strength of CEM III can reach up to 180% of the 28-day strength under normal conditions.
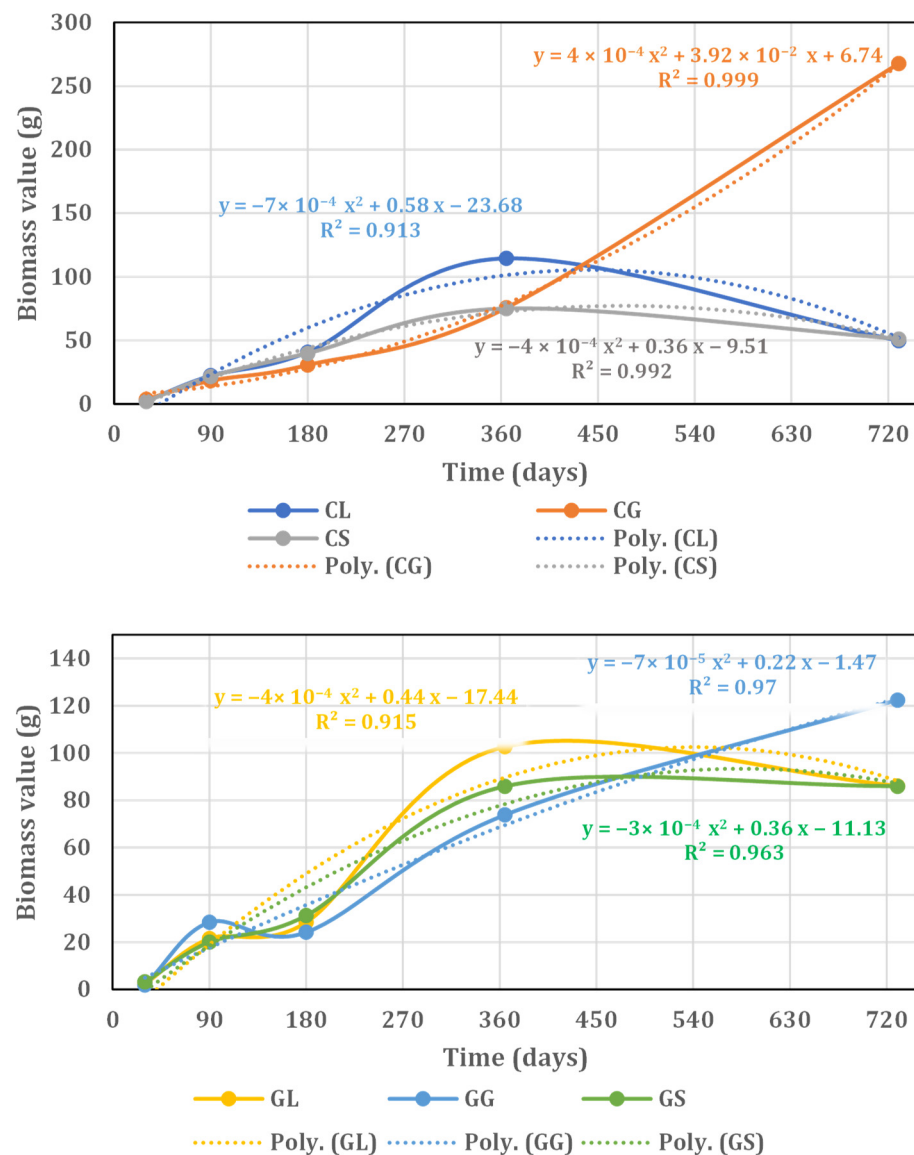
The first chart shows biomass value (g) versus time (days) for CL, CG, CS and their polynomial fits:

$$y = 4 \times 10^{-4} x^2 + 3.92 \times 10^{-2}\ x + 6.74$$
$$R^2 = 0.999$$

$$y = -7 \times 10^{-4}\ x^2 + 0.58\ x - 23.68$$
$$R^2 = 0.913$$

$$y = -4 \times 10^{-4}\ x^2 + 0.36\ x - 9.51$$
$$R^2 = 0.992$$

The second chart shows biomass value (g) versus time (days) for GL, GG, GS and their polynomial fits:

$$y = -7 \times 10^{-5}\ x^2 + 0.22\ x - 1.47$$
$$R^2 = 0.97$$

$$y = -4 \times 10^{-4}\ x^2 + 0.44\ x - 17.44$$
$$R^2 = 0.915$$

$$y = -3 \times 10^{-4}\ x^2 + 0.36\ x - 11.13$$
$$R^2 = 0.963$$

Figure 10. Biomass evolution over time of immersion.

Figures 12–14 show the regression model of flexural strength, compressive strength, and Young's modulus, respectively. The regression model of the average of all the samples represents very well the behavior of the studied materials. These models present the attenuation in term of mechanical strengths and the Young's modulus with the time of immersion. Regarding the tensile strength, an increase was observed for CL and CS while a decrease was noted for the other formulations generally. For CL and CS formulations, a slight decrease was noted after one year of immersion for CL and after 6 months for CS. Concerning the compressive strength, an increase was noted after 3 months of immersion by 27%, 33%, 37%, 25%, 10%, and 20% compared to the results of 1 month of immersion for CL, CG, CS, GL, GG, and GS respectively. This increase is explained by the pozzolanic activity of the binders used. Beyond that, a decrease was noted and may be explained by the change in pH of the samples which affects the hydration process. In general, a decrease was observed according to the time of immersion and this can vary up to −25% for CL and CG, −67% for GL, and −40% for GL and GS which show the same behavior. While CS showed an increase of 16% at 3 months of immersion compared to the results of 1 month, this was followed by a decrease of 6% at 6 months of immersion compared to the results of 1 month. After 6 months, a stabilization was noticed along the time immersion.
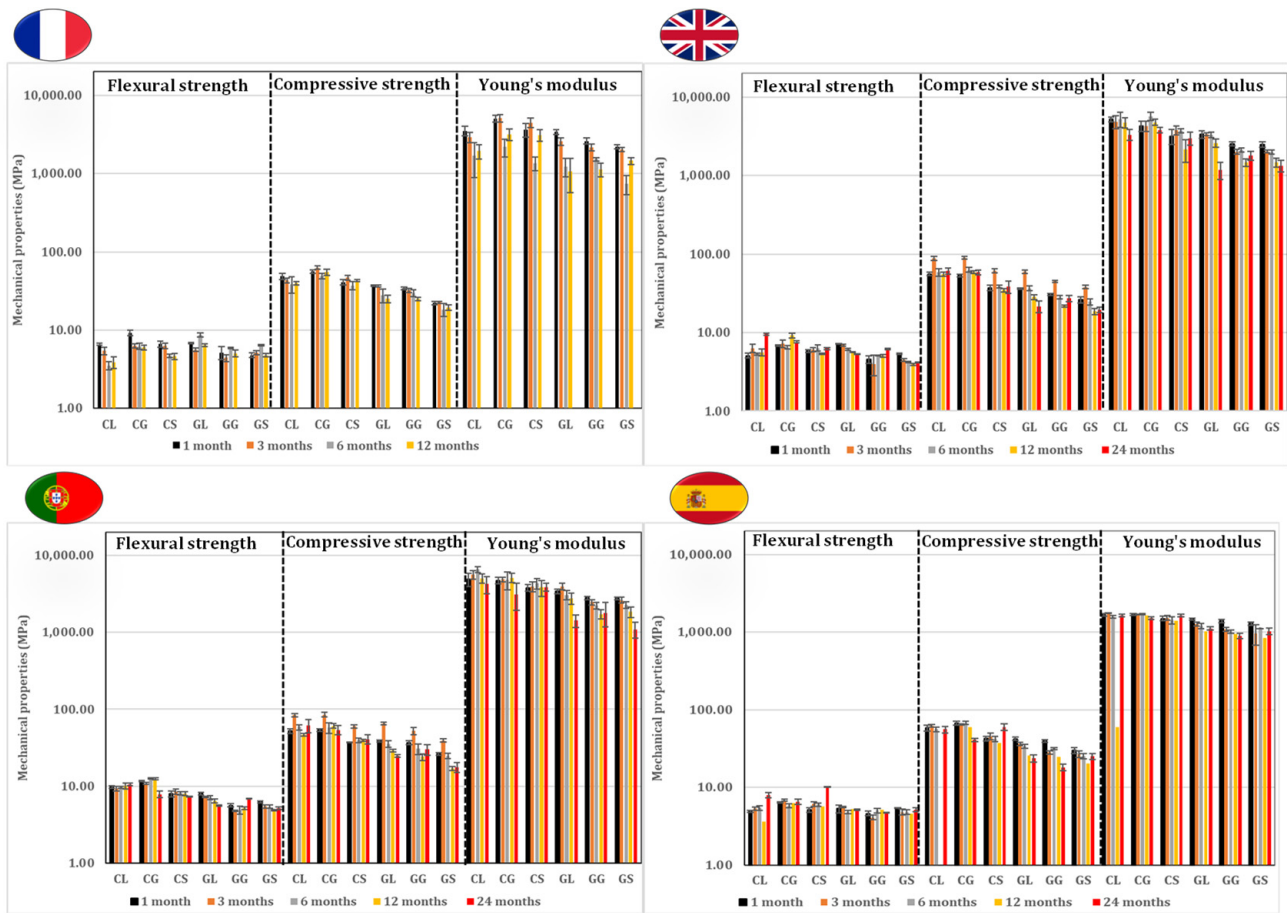
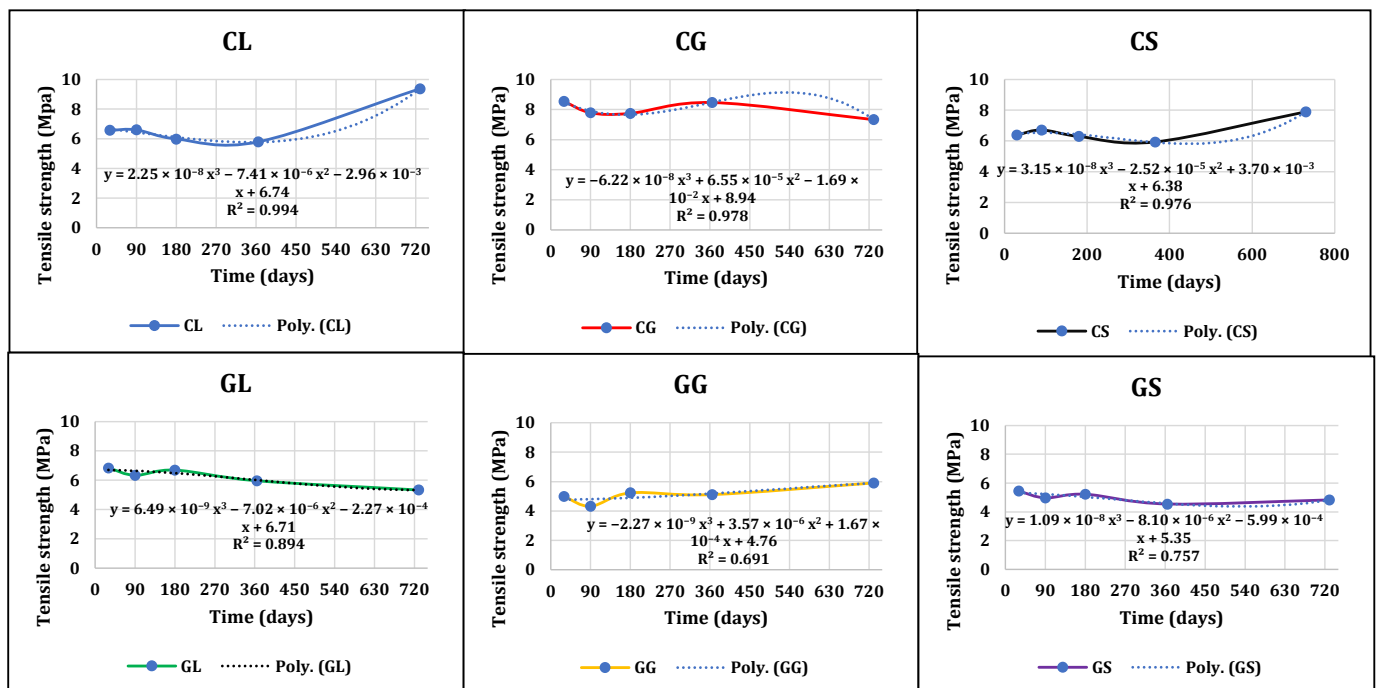**Figure 11.** Mechanical properties of studied materials at 1, 3, 6, 12, and 24 months.

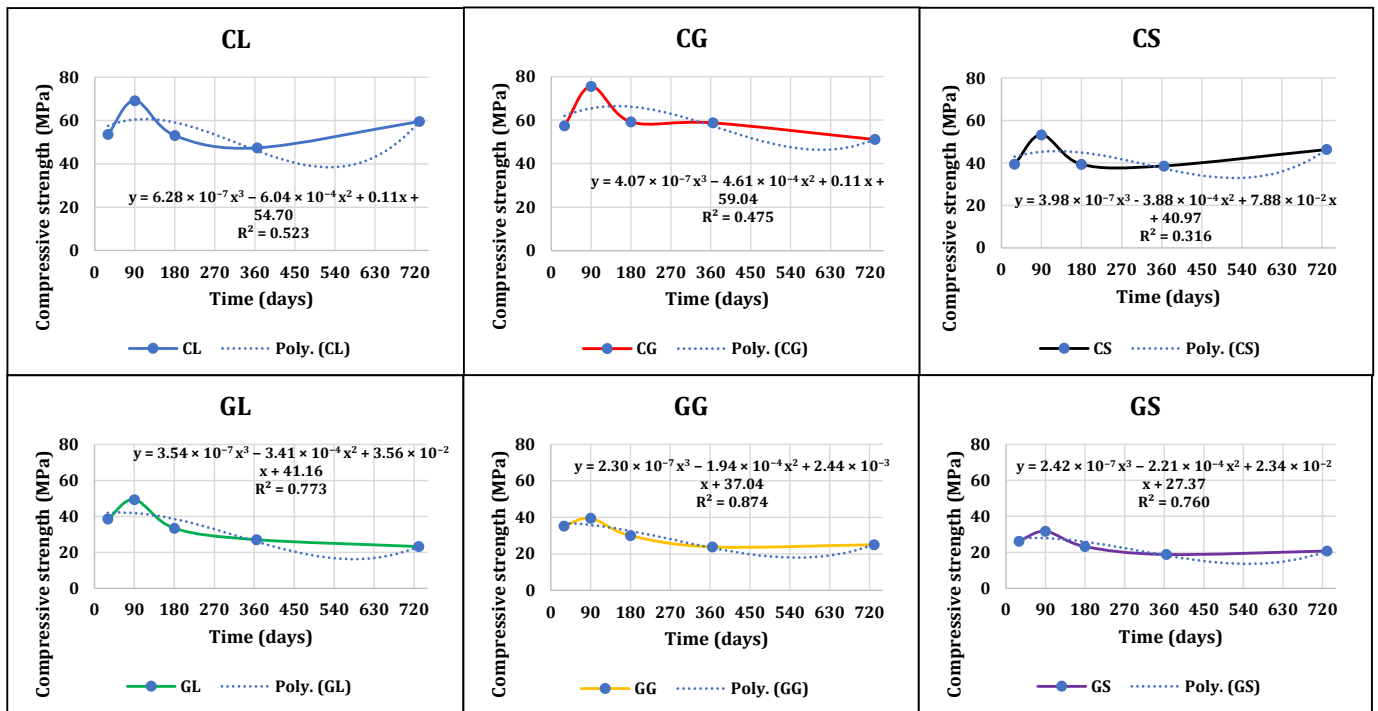**Figure 12.** Tensile strength evolution during the immersion of studied materials.

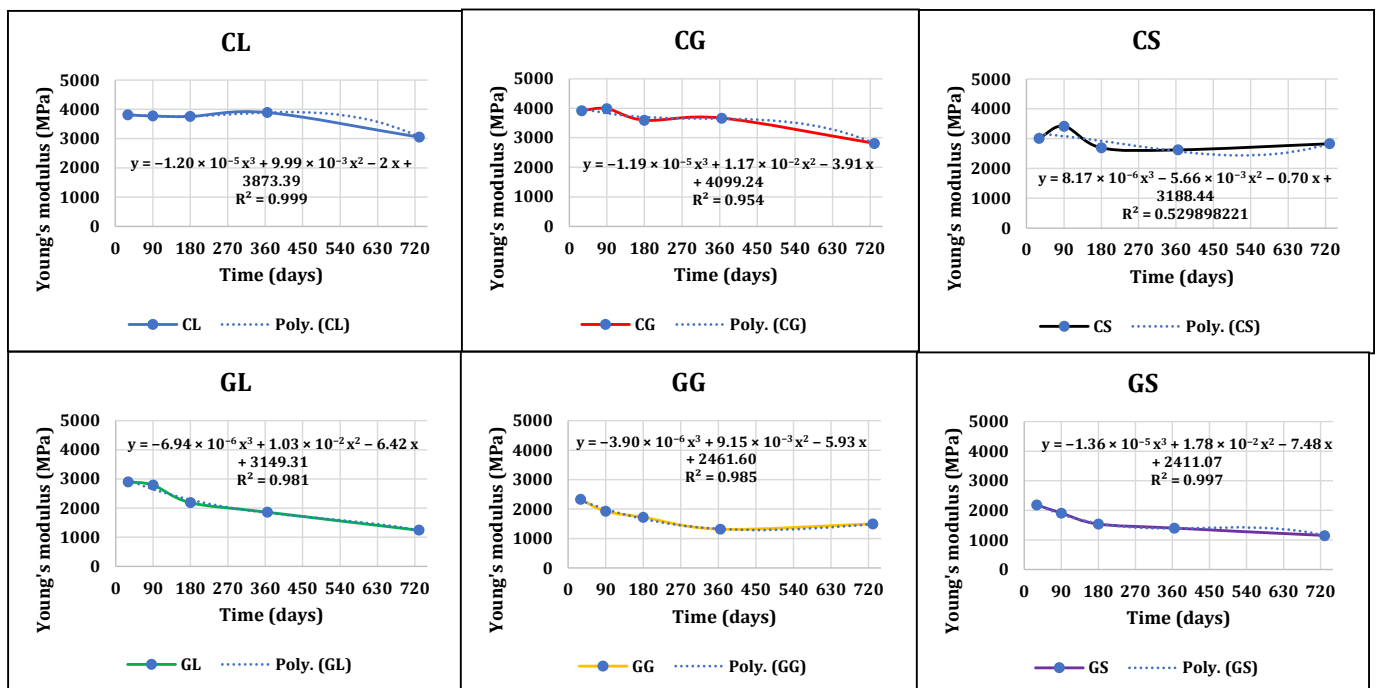**Figure 13.** Compressive strength of studied materials.

Figure 14. Young's modulus of studied materials.

4. Conclusions

An experimental study was carried out on the properties evolution of eco-material dedicated to manufacturing artificial reef via 3D printing. This experimental campaign considers the effect of raw materials and region of immersion on its mechanical and durability properties, namely the tensile and compressive strengths, the Young's modulus, and the biomass colonization. The relevant conclusions can be drawn:

- CL and CG formulations show the higher value in terms of mechanical properties and bio-colonization mass.
- Formulations based on CEM III presented better results than those based on geopolymer.
- A decrease of the mechanical properties with the immersion duration was observed.
- Due to the interaction between the cementitious materials and marine environment, an increase of bio-colonization mass was noticed until one year of immersion, after which a decrease was noted.

The experimental characterization campaign reported in this work has not only enriched the database of material properties but has also supplied the formulation optimized to manufacture the artificial reefs. Therefore, further investigation will be achieved to highlight the advantages of using these materials in terms of durability and the environmental impacts.

References

1. Hess, R.W.; Hynes, M.V.; Peters, J.E. *Disposal Options for Ships*; 2001. [CrossRef]
2. Crain, C.M.; Halpern, B.S.; Beck, M.W.; Kappel, C.V. Understanding and Managing Human Threats to the Coastal Marine Environment. *Ann. N. Y. Acad. Sci.* **2009**, *1162*, 39–62. [CrossRef] [PubMed]
3. Baine, M. Artificial reefs: A review of their design, application, management and performance. *Ocean Coast. Manag.* **2001**, *44*, 241–259. [CrossRef]
4. Reis, B.; van der Linden, P.; Pinto, I.S.; Almada, E.; Borges, M.T.; Hall, A.E.; Stafford, R.; Herbert, R.J.H.; Lobo-Arteaga, J.; Gaudêncio, M.J.; et al. Artificial reefs in the North –East Atlantic area: Present situation, knowledge gaps and future perspectives. *Ocean Coast. Manag.* **2021**, *213*, 105854. [CrossRef]
5. Firth, L.; Knights, A.; Bridger, D.; Evans, A.; Mieszkowska, N.; Moore, P.; O'connor, N.; Sheehan, E.; Thompson, R.; Hawkins, S. Ocean Sprawl: Challenges and Opportunities for Biodiversity Management in A Changing World. In *Oceanography and Marine Biology*; CRC Press: Boca Raton, FL, USA, 2016; pp. 193–270. [CrossRef]
6. Schygulla, C.; Peine, F. Nienhagen reef: Abiotic boundary conditions at a large brackish water artificial reef in the baltic sea. *J. Coast. Res.* **2013**, *29*, 478–486. [CrossRef]
7. Spagnolo, A.; Cuicchi, C.; Punzo, E.; Santelli, A.; Scarcella, G.; Fabi, G. Patterns of colonization and succession of benthic assemblages in two artificial substrates. *J. Sea Res.* **2014**, *88*, 78–86. [CrossRef]
8. Charbonnel, E.; Carnus, F.; Ruitton, S.; le Direac'h, L.; Harmelin, J.-G.; Beurois, J. Artificial Reefs in Marseille: From Complex Natural Habitats to Concepts of Efficient Artificial Reef Design. In *Global Change: Mankind-Marine Environment Interactions*; Springer: Dordrecht, The Netherlands, 2010; pp. 81–82. [CrossRef]

9. Ramos, J.; Lino, P.G.; Himes-Cornell, A.; Santos, M.N. Local fishermen's perceptions of the usefulness of artificial reef ecosystem services in Portugal. *Peer J.* **2019**, *6*, e6206. [CrossRef] [PubMed]

10. Kruth, J.-P.; Leu, M.C.; Nakagawa, T. Progress in Additive Manufacturing and Rapid Prototyping. *Cirp Ann.* **1998**, *47*, 525–540. [CrossRef]

11. Chu, C.; Graf, G.; Rosen, D.W. Design for Additive Manufacturing of Cellular Structures. *Comput. Aided Des. Appl.* **2008**, *5*, 686–696. [CrossRef]

12. Gero, J.S. Recent Advances in Computational Models of Creative Design. In *Computing in Civil and Building Engineering*; Pahl, P., Werner, H., Eds.; Balkema: Rotterdam, The Netherlands, 1995; pp. 21–30. Available online: https://cs.gmu.edu/~{}jgero/publications/1996.html (accessed on 8 June 2022).

13. Cesaretti, G.; Dini, E.; de Kestelier, X.; Colla, V.; Pambaguian, L. Building components for an outpost on the Lunar soil by means of a novel 3D printing technology. *Acta Astronaut.* **2014**, *93*, 430–450. [CrossRef]

14. Lloret, E.; Shahab, A.R.; Linus, M.; Flatt, R.J.; Gramazio, F.; Kohler, M.; Langenberg, S. Complex concrete structures. *Comput. Des.* **2015**, *60*, 40–49. [CrossRef]

15. Pegna, J. Exploratory investigation of solid freeform construction. *Autom. Constr.* **1997**, *5*, 427–437. [CrossRef]

16. Lowke, D.; Dini, E.; Perrot, A.; Weger, D.; Gehlen, C.; Dillenburger, B. Particle-bed 3D printing in concrete construction—Possibilities and challenges. *Cem. Concr. Res.* **2018**, *112*, 50–65. [CrossRef]

17. Kazemian, A.; Yuan, X.; Cochran, E.; Khoshnevis, B. Cementitious materials for construction-scale 3D printing: Laboratory testing of fresh printing mixture. *Constr. Build. Mater.* **2017**, *145*, 639–647. [CrossRef]

18. Le, T.T.; Austin, S.A.; Lim, S.; Buswell, R.A.; Gibb, A.G.F.; Thorpe, T. Mix design and fresh properties for high-performance printing concrete. *Mater. Struct.* **2012**, *45*, 1221–1232. [CrossRef]

19. Ma, G.; Wang, L. A critical review of preparation design and workability measurement of concrete material for largescale 3D printing. *Front. Struct. Civ. Eng.* **2018**, *12*, 382–400. [CrossRef]

20. Perrot, A.; Mélinge, Y.; Rangeard, D.; Micaelli, F.; Estellé, P.; Lanos, C. Use of ram extruder as a combined rheo-tribometer to study the behaviour of high yield stress fluids at low strain rate. *Rheol. Acta* **2012**, *51*, 743–754. [CrossRef]

21. Cépralmar, Région Languedoc-Roussillon – 21 avril 2015 - Guide Pratique D'aide à L'élaboration, L'exploitation et la Gestion des Récifs Artificiels en Languedoc-Roussillon: 236 pages. Available online: https://pole-lagunes.org/guide-pratique-daide-a-lelaboration-lexploitation-et-la-gestion-des-recifs-artificiels-en-languedoc-roussillon/ (accessed on 8 June 2022).

22. Yoris-Nobile, A.I.; Lizasoain-Arteaga, E.; Slebi-Acevedo, C.J.; Blanco-Fernandez, E.; Alonso-Cañon, S.; Indacoechea-Vega, I.; Castro-Fresno, D. Life cycle assessment (LCA) and multi-criteria decision-making (MCDM) analysis to determine the performance of 3D printed cement mortars and geopolymers. *J. Sustain. Cem. Mater.* **2022**, 1–18. [CrossRef]

23. Ly, O.; Yoris-Nobile, A.I.; Sebaibi, N.; Blanco-Fernandez, E.; Boutouil, M.; Castro-Fresno, D.; Hall, A.E.; Herbert, R.J.H.; Deboucha, W.; Reis, B.; et al. Optimisation of 3D printed concrete for artificial reefs: Biofouling and mechanical analysis. *Constr. Build. Mater.* **2021**, *272*, 121649. [CrossRef]

24. *NF EN196–1*; Methods of testing cement—Part 1: Determination of strength. AFNOR edition; CEN: Paris, France, 2016.

25. El-Khoury, M.; Roziere, E.; Grondin, F.; Cortas, R.; Chehade, F.H. Experimental evaluation of the effect of cement type and seawater salinity on concrete offshore structures. *Constr. Build. Mater.* **2022**, *322*, 126471. [CrossRef]

26. Hayek, M.; Salgues, M.; Habouzit, F.; Bayle, S.; Souche, J.-C.; de Weerdt, K.; Pioch, S. In vitro and in situ tests to evaluate the bacterial colonization of cementitious materials in the marine environment. *Cem. Concr. Compos.* **2020**, *113*, 103748. [CrossRef]

27. Boukhelf, F.; Cherif, R.; Trabelsi, A.; Belarbi, R.; Bouiadjra, M.B. On the hygrothermal behavior of concrete containing glass powder and silica fume. *J. Clean. Prod.* **2021**, *318*, 128647. [CrossRef]

28. Sebaibi, N.; Benzerzour, M.; Abriak, N.-E.; Binetruy, C. Mechanical and physical properties of a cement matrix through the recycling of thermoset composites. *Constr. Build. Mater.* **2012**, *34*, 226–235. [CrossRef]

29. Zeng, H.; Li, Y.; Zhang, J.; Chong, P.; Zhang, K. Effect of limestone powder and fly ash on the pH evolution coefficient of concrete in a sulfate-freeze–thaw environment. *J. Mater. Res. Technol.* **2022**, *16*, 1889–1903. [CrossRef]

30. Polder, R.B.; Peelen, W.H. Characterisation of chloride transport and reinforcement corrosion in concrete under cyclic wetting and drying by electrical resistivity. *Cem. Concr. Compos.* **2002**, *24*, 427–435. [CrossRef]

31. Mittermayr, F.; Rezvani, M.; Baldermann, A.; Hainer, S.; Breitenbücher, P.; Juhart, J.; Graubner, C.-A.; Proske, T. Sulfate resistance of cement-reduced eco-friendly concretes. *Cem. Concr. Compos.* **2015**, *55*, 364–373. [CrossRef]

32. Osmanovic, Z.; Haračić, N.; Zelić, J. Properties of blastfurnace cements (CEM III/A, B, C) based on Portland cement clinker, blastfurnace slag and cement kiln dusts. *Cem. Concr. Compos.* **2018**, *91*, 189–197. [CrossRef]